6 Relevant Topographic Anatomy of the Head, Anatomical Variants, and Risk Zones

Ximena Wortsman and Camila Ferreira-Wortsman

Introduction

This chapter analyzes the most relevant points in the head anatomy, particularly the facial anatomy and the submandibular regions. In addition, we highlight the anatomical structures that may be potentially involved or injured during surgical or cosmetic procedures.

Relevant Topographic Anatomy of the Head

Facial Anatomy

The knowledge of facial anatomy is crucial for the performance of dermatologic procedures. This is due to the high rate of involvement of the face in multiple dermatologic conditions, including skin cancer and common aesthetic procedures performed in the face. Thus, several critical anatomical regions should be reviewed, such as facial muscles, eyelids, nose, lips, and ears.

Knowledge of the surface anatomy is also essential to understand the pathophysiology of aging and the clinical language for requesting the ultrasonographic examinations. Additionally, it is necessary to keep in mind the main expression lines and wrinkles of the face (Fig. 6.1) and the main anatomical layers of the face (Fig. 6.2).

Fig. 6.1 Frequent facial wrinkles and expression lines

X. Wortsman (✉)
Institute for Diagnostic Imaging and Research of the Skin and Soft Tissues, Santiago, RM, Chile

Department of Dermatology, Universidad de Chile, Santiago, RM, Chile

Department of Dermatology, Pontificia Universidad Catolica de Chile, Santiago, RM, Chile

C. Ferreira-Wortsman
School of Medicine, Universidad Finis Terrae, Santiago, Chile

X. Wortsman (ed.), *Textbook of Dermatologic Ultrasound*,
https://doi.org/10.1007/978-3-031-08736-3_6

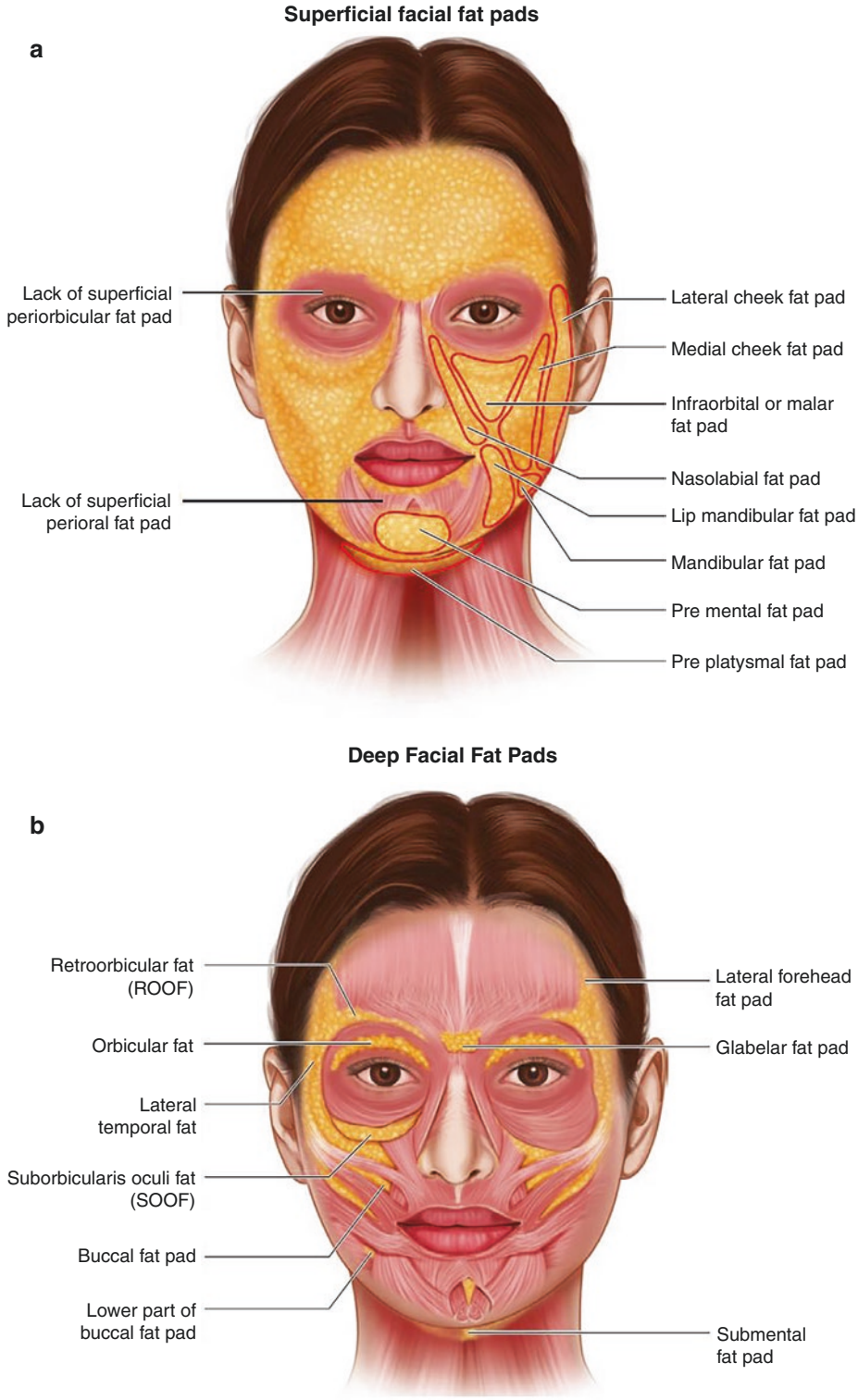

Fig. 6.2 Drawings of facial anatomy. (**a**) Superficial fat pads of the face. (**b**) Deep fat pads of the face. (**c**) Muscles of the face. Abbreviations: *ROOF* retro-orbicularis oculi fat, *SOOF* suborbicularis oculi fat

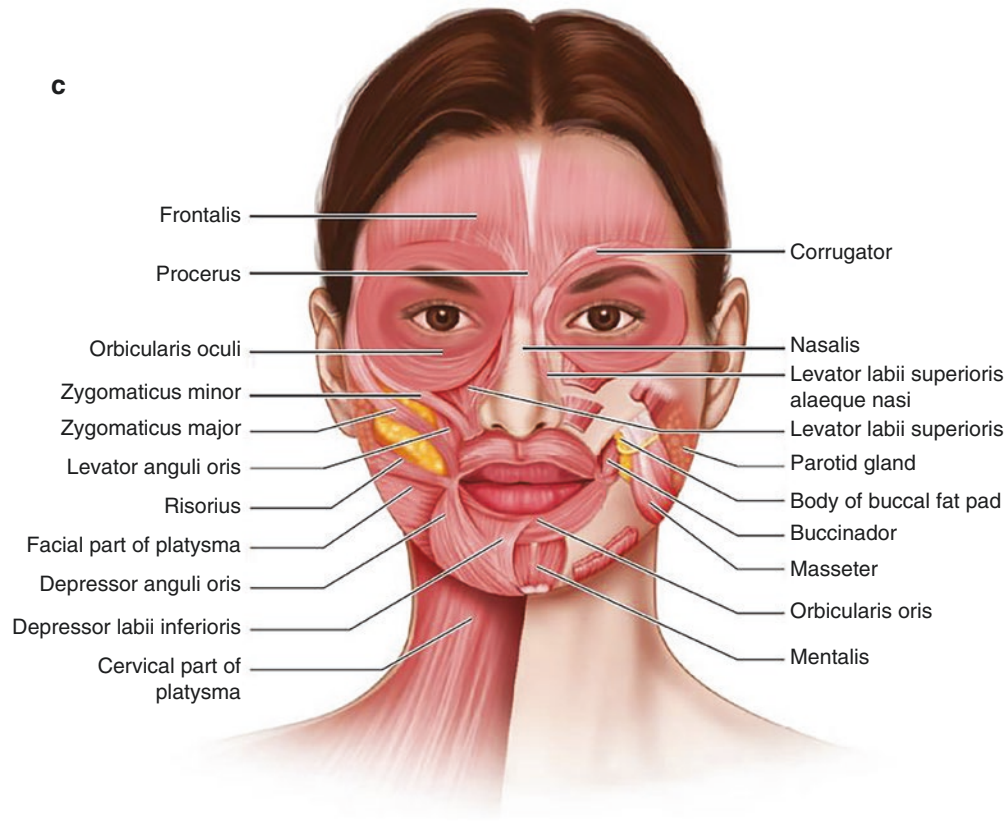

Fig. 6.2 (continued)

Muscles of the Face

The musculoaponeurotic layer of the face contains multiple muscles, some of them very thin, such as the orbicularis or the peribuccal muscles; however, there are thick muscles such as the masseter muscles. The most important muscles of the face with their insertions are described in Table 6.1. The probe's location for observing these muscles and their ultrasonographic appearance are shown in Figs. 6.3, 6.4, 6.5, 6.6, 6.7, 6.8, 6.9, 6.10, 6.11, 6.12, 6.13, 6.14, and 6.15.

All muscles appear as hypoechoic band-like structures of variable thicknesses. For scanning these muscles, it is necessary to find their axes to locate the probe properly [1–19].

Eyelids

The upper and lower eyelids are complex structures. Each of them can be divided for academic purposes into three layers. The anterior layer is composed of the epidermis and dermis, with some hair follicles, more commonly found in the upper eyelid. The orbicularis muscle is the middle layer, and the posterior layer, also called the tarsal plate, mainly contains multiple acinar structures of Meibomian glands.

The epidermis, dermis, and hair follicles maintain the ultrasonographic structure already described in previous chapters.

The orbicularis muscle appears as a hypoechoic band that surrounds the eye. This band can show upward displacement under the contraction of the muscle. The Meibomian glands present as rows of hyperechoic oval-shaped structures disposed in a vertical shape. In the eyelids' medial part, it is possible to detect the upper and lower lacrimal canaliculi that drain the tears to the nasolacrimal sac in the medial part of the

Table 6.1 Main muscles of the face origins, insertions, and actions

Muscle name	Origin	Insertion	Actions	Comments	Wrinkles
Frontalis or epicranius	Galea aponeurotica	Orbicularis oculi muscle, procerus muscle	Raise eyebrows	No bony attachment	Horizontal forehead lines
				88% individuals show bifurcation	
				46% of these 88% with microscopic muscle fibers at the bifurcation and beyond	
Corrugator	Medial supraorbital rim 46%	Medial half of brow skin	Frowning, angry expressions	Pull medial part of eyebrows together	Vertical glabellar or frown lines
	Medial frontal bone 31%				
	Medial infraorbital rim 17%				
	Upper nasal process 7%				
Orbicularis oculi	Frontal bone	Fibrofatty tissue eyelid	Orbital part: close eyelids voluntarily	It has 3 parts	Crow´s feet lines
	Maxillary bone		Palpebral part: close eyelids involuntarily	Orbital orbicularis: ellipse-shaped, outer	Tear throughs
			Reflex blinking	Palpebral orbicularis: upper and lower eyelids	Nasojugal groove
			Lacrimal part: compresses the lacrimal sac	Lacrimal orbicularis or tensor tarsi	
				Antagonist: levator palpebrae superioris	
Procerus	Fascia on top of nasal bones	Fibrofatty glabellar tissue, frontal fascia	Frowning downward	Pull medial part of eyebrows downward	Horizontal or bunny lines
			Very angry expressions	Flaring nostrils	
				Pyramid-shaped	
Zygomaticus major	Zygomatic bone	Modiolus	Smiling	Raise angle of the mouth upward and laterally	Nasolabial lines
				34% can show a bifid structure lateral to the zygomatic minor muscle	Midcheek lines or furrows
Zygomaticus minor	Zygomatic bone	Fibrofatty hypodermal tissue	Sad facial expressions	Upper lip backward, upward, and outward prominent fibrous component	Nasolabial lines
Levator labii superioris	Medial infraorbitary margin	Orbicularis oris	Elevation of the upper lip	Some fibers merge with the procerus	Vertical lines upper lip
		Fibrofatty tissue of the upper lip			nasolabial lines
Levator labii superioris	Nasal bones	Lateral fibrofatty tissue nostrils	Dilation of nostrils	Merge with fibers of the nasalis muscle	Nasojugal groove

Table 6.1 (continued)

Muscle name	Origin	Insertion	Actions	Comments	Wrinkles
Alaeque nasi		Upper lip	Elevation of the upper lip	Due to its action it has been called "Elvis muscle" in remembrance of the expressions commonly performed by the singer Elvis Presley, it is attached to the medial part of the maxillary bone	
			Elevation of the wing of the nose		
Levator anguli oris	Maxillary bone canine fossa	Modiolus	Smiling elevation of the upper lip	Also called caninus muscle	
Risorius	Parotid fascia	Modiolus	Lateral smiling pulls backward the angles of the mouth	Thin bundle with prominent fibrous component may partially cover the masseter muscle	
	Masseter fascia, platysma				
Orbicularis oris	Maxilla, mandible	Fibrofatty tissue of the lips	Puckering the lips, kissing	Circle-shaped muscle connected to other muscles in the modiolus region	Vertical upper lip lines
Depressor anguli oris	Tubercle of manndible	Modiolus	Lower and lateral displacement of the angles of the mouth, sadness expression	Also called triangular muscle	Marionette lines
Depressor labii inferioris	Oblique line of mandible	Fibrofatty tissue of the lower lip	Depression of lower lip sadness	Also called quadratus fibers blend with orbicularis oris	
Mentalis	Anterior mandible	Fibrofatty tissue of the lower lip	Protrusion lower lip, elevation of the soft tissues of the chin, pout expression	Paired muscle	Crease lines at the chin
Masseter	Zygomatic arch, maxillary process of the zygomatic bone	Angle and lateral surface of the ramus of the mandible, coronoid process	Mastication	Elevation of the mandible necessary for closing the mouth	
				Hypertrophy affects the lateral shape of the lower face	
Platysma	Fibrofatty tissue of the infraclavicular and acromial regions	Anterior and lateral parts of the mandible, fibrofatty tissue of the chin	Lower the mandible and corners of the mouth stress or tension expression in the face and neck	Thin band of muscle that overlaps the sternocleidomastoid	Marionette lines

(continued)

Table 6.1 (continued)

Muscle name	Origin	Insertion	Actions	Comments	Wrinkles
				Pectoralis major and deltoid muscles	Medial neck vertical lines
			Sadness expression		Chin crease or dimpling
Nasalis	Medial aspect of the maxilla	Nasal bones	Elevation of the nostrils	Its has 2 parts	
			Depression of the tip of the nose	Transverse part : covers the bridge of the nose	
			Compression of the bridge of the nose	Alar part: attached to the alar cartilages	

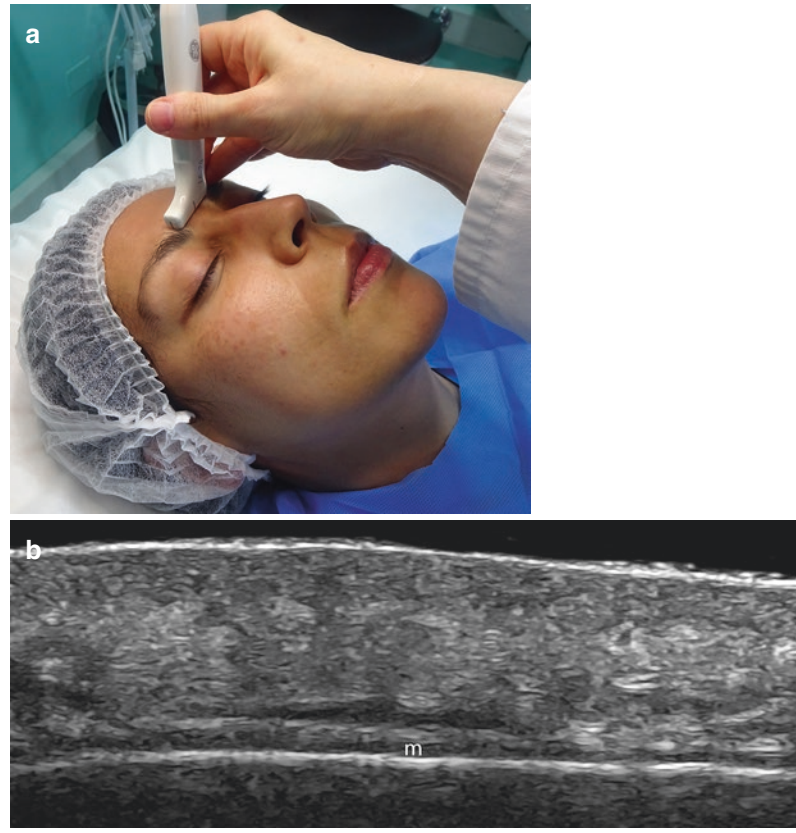

Fig. 6.3 Frontalis muscle. (**a**) Clinical image shows the location of the probe. (**b**) Ultrasound image (grayscale, transverse view) demonstrates the frontalis muscle (m)

upper and lower eyelids. The latter structures are more evident at 70 MHz or when they are dilated and appear as anechoic tubules.

The vascularity of the eyelids comes from anastomoses from the internal carotid via terminal branches of the ophthalmic (supraorbital, supratrochlear, and dorsal nasal) and lacrimal arteries with terminal branches of vessels derived from the external carotid system, so it gathers branches that come from the facial, angular, superficial temporal, and infraorbital arteries. Of the four main branches of the superficial tempo-

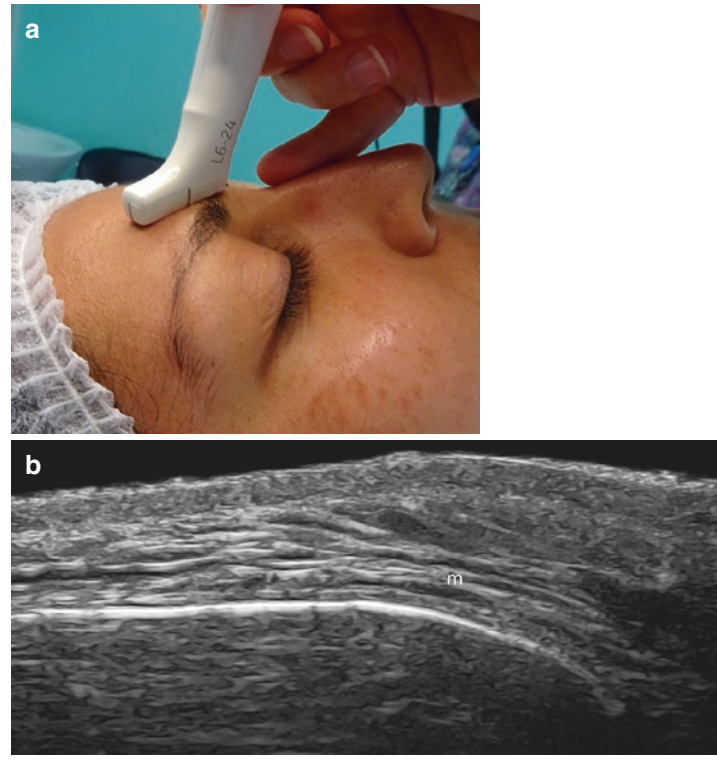

Fig. 6.4 Corrugator muscle. (**a**) Clinical image presents the location of the probe. (**b**) Ultrasound (grayscale; oblique view) shows the corrugator muscle (m)

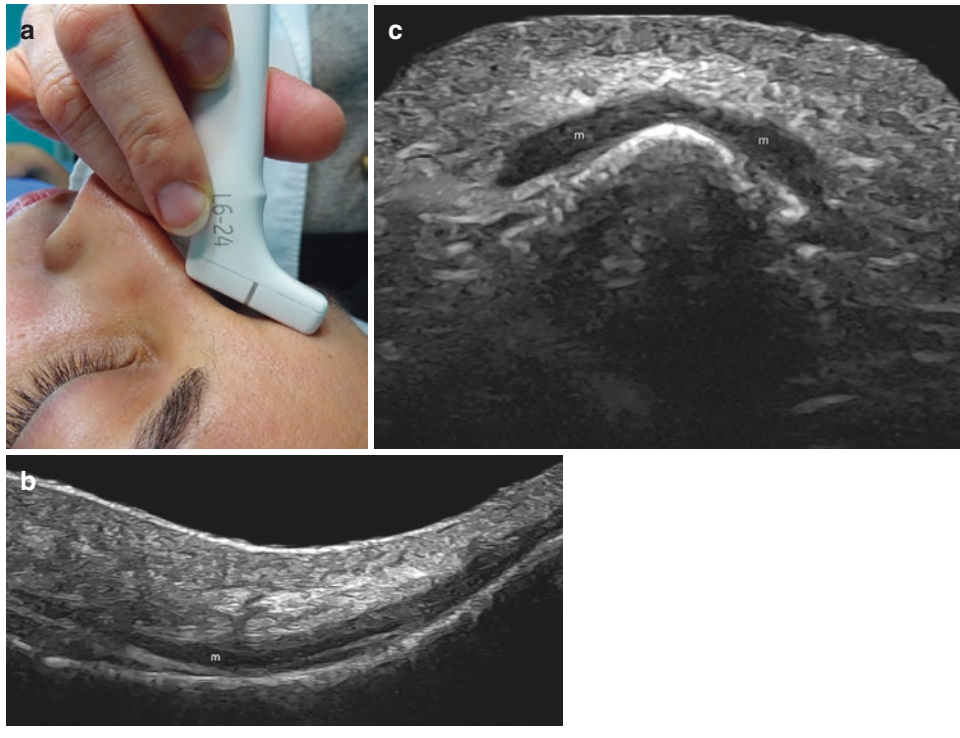

Fig. 6.5 Procerus muscles. (**a**) Clinical photograph demonstrates the probe's location. Ultrasound images (grayscale; **b**, longitudinal; **c**, transverse) show the procerus muscles (m)

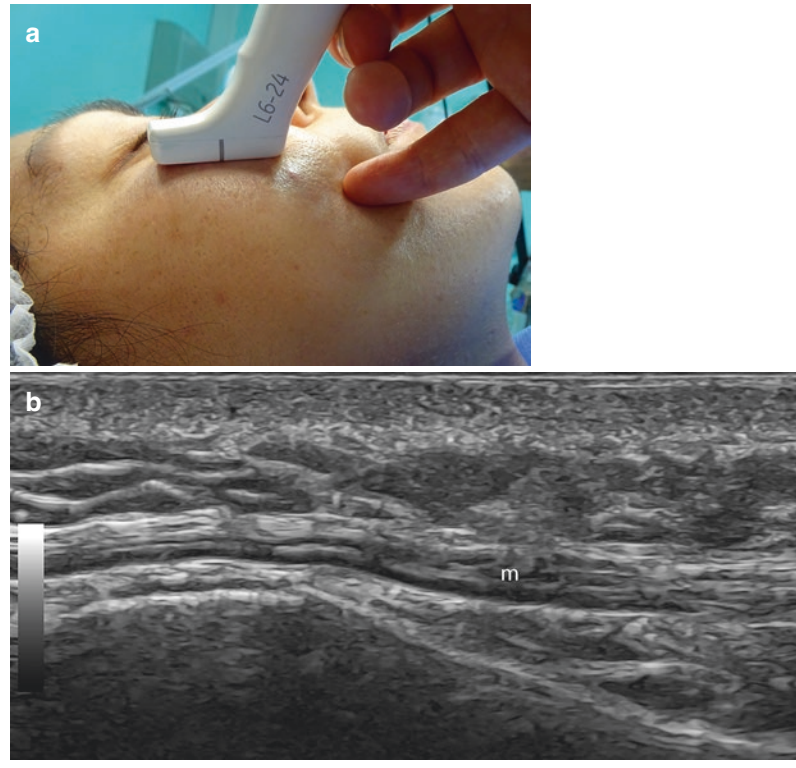

Fig. 6.6 Zygomaticus major muscle. (**a**) Clinical image shows the location of the probe. (**b**) Ultrasound image demonstrates the zygomaticus major muscle (m)

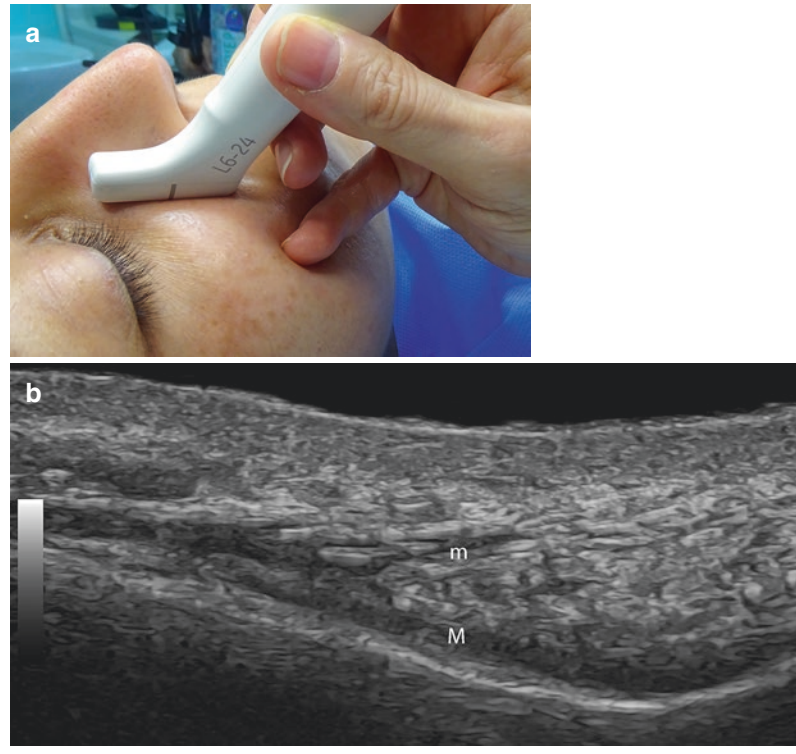

Fig. 6.7 Levator labii superioris and levator labii superioris alaeque nasi muscles. (**a**) Clinical image presents the location of the probe. (**b**) Ultrasound (grayscale) demonstrates both the muscles. The levator labii superioris muscle (M) is deeper than the levator labii superioris alaeque nasi muscle (m)

Fig. 6.8 Modiolus region. This is a junction zone of the following muscles: zygomaticus major, buccinator, platysma pars modiolaris, pars marginalis orbicularis oris, levator anguli oris, mentalis, depressor labii inferioris, depressor anguli oris, and risorius (**a**) Clinical photograph demonstrates the location of the probe. (**b**) Ultrasound image (grayscale) shows the modiolus region (m)

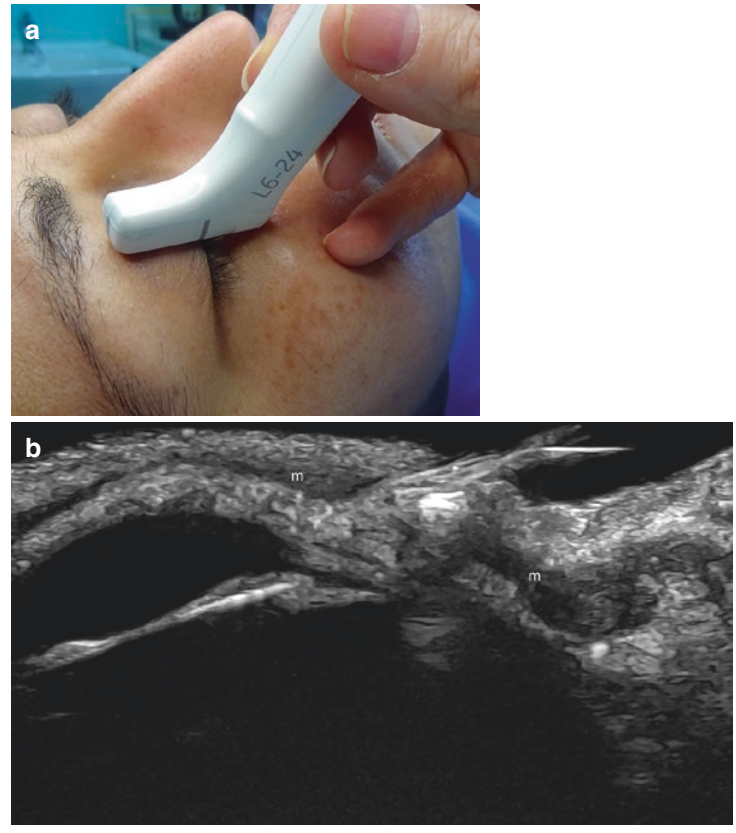

Fig. 6.9 Orbicularis oculi muscle of the eyelids. (**a**) Clinical image demonstrates the position of the probe. (**b**) Ultrasound image (grayscale, longitudinal view) presents the upper (left) and lower (right) orbicularis oculi muscles (m) of the eyelids (palpebral parts)

Fig. 6.10 Orbicularis oris of the lips. (**a**) Clinical photograph shows the probe's location. (**b**) Ultrasound image (grayscale, longitudinal view) presents the upper (left) and lower (right) orbicularis oris muscle (m) of the lips

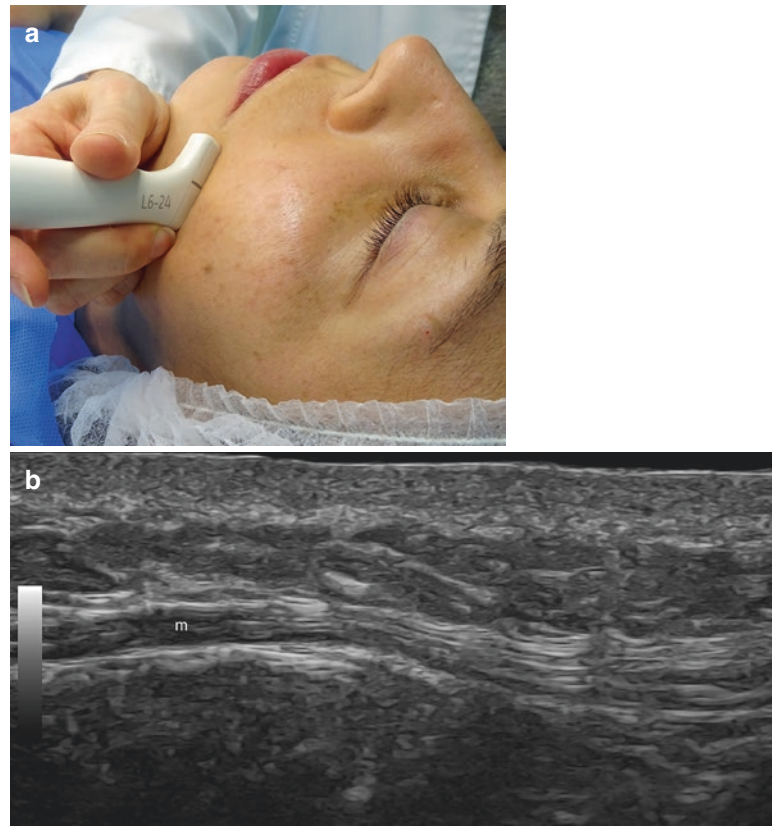

Fig. 6.11 Risorius muscle. (**a**) Clinical photograph demonstrates the location of the probe. (**b**) Ultrasound image (grayscale; longitudinal axis of the muscle) presents the risorius muscle (m)

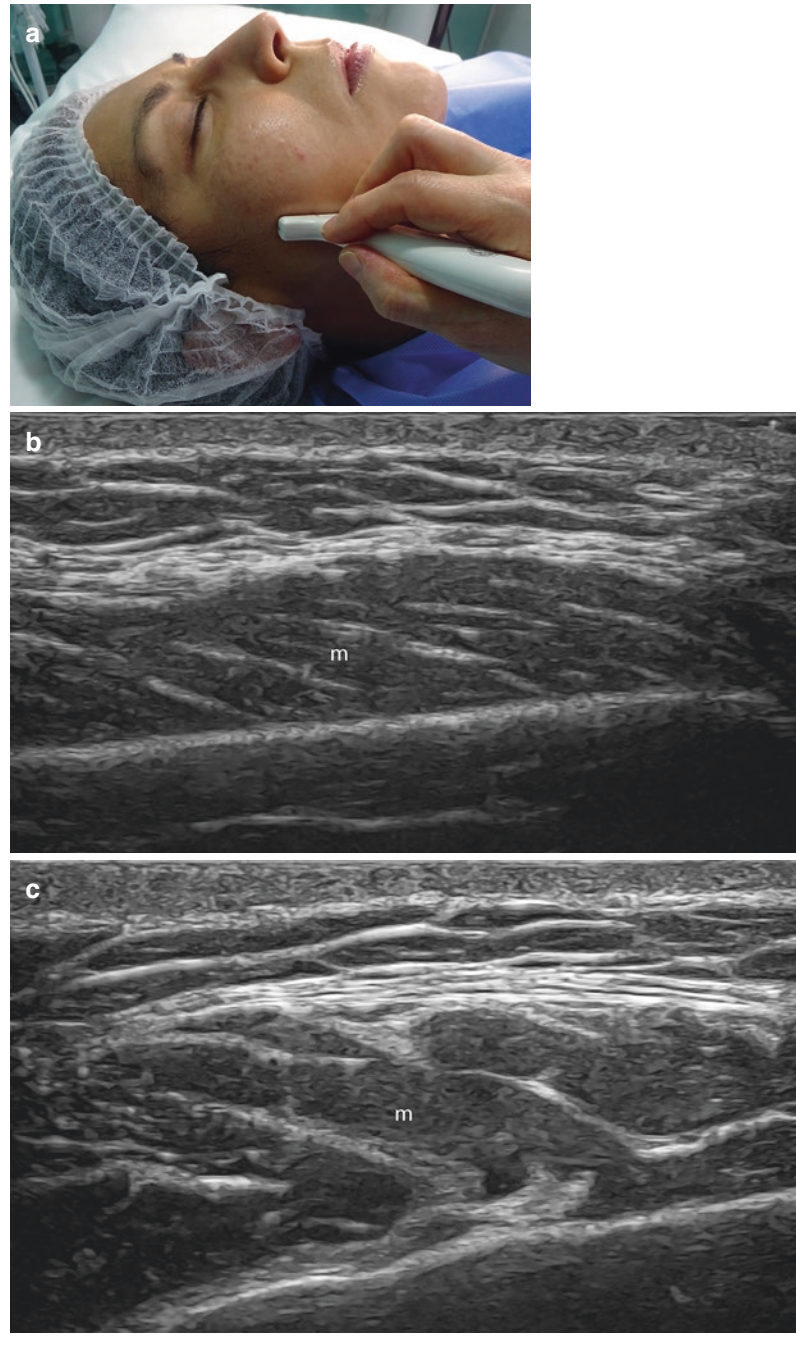

Fig. 6.12 Masseter muscle. (**a**) Clinical photograph demonstrates the location of the probe for the acquisition of the ultrasound images (**b**, **c**). Ultrasound images show the masseter muscle (m) in longitudinal (**b**) and transverse (**c**) views on top of the mandible

ral artery (transverse facial, frontal, middle temporal, and parietal), the transverse facial and frontal branches contribute significantly to eyelid vascularity and anastomose with their counterparts on the opposite side, as well as with the supraorbital artery (Fig. 6.16a–d).

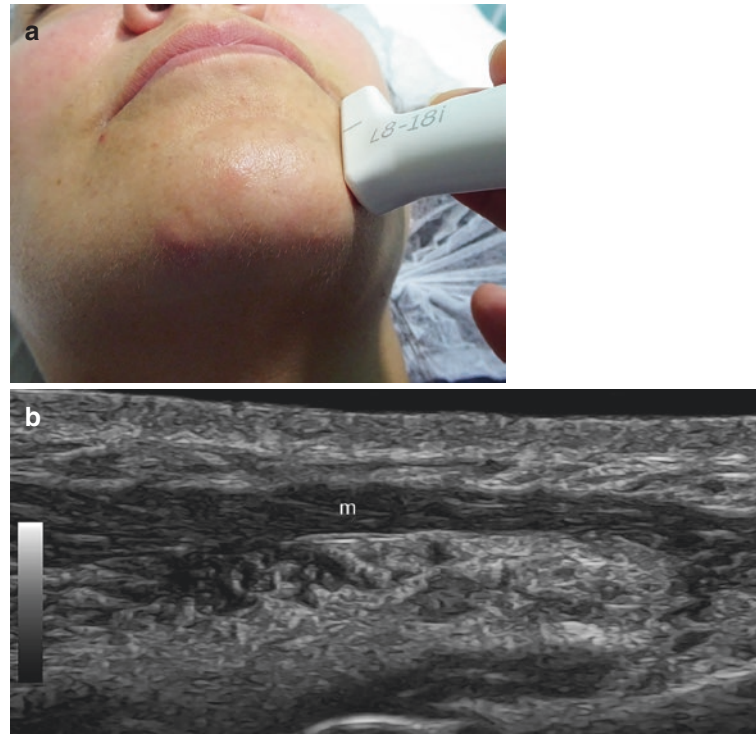

Fig. 6.13 Depressor anguli oris muscle. (**a**) Clinical image shows the probe's location. (**b**) Ultrasound (grayscale, longitudinal view of the muscle) demonstrates the depressor anguli oris muscle (m)

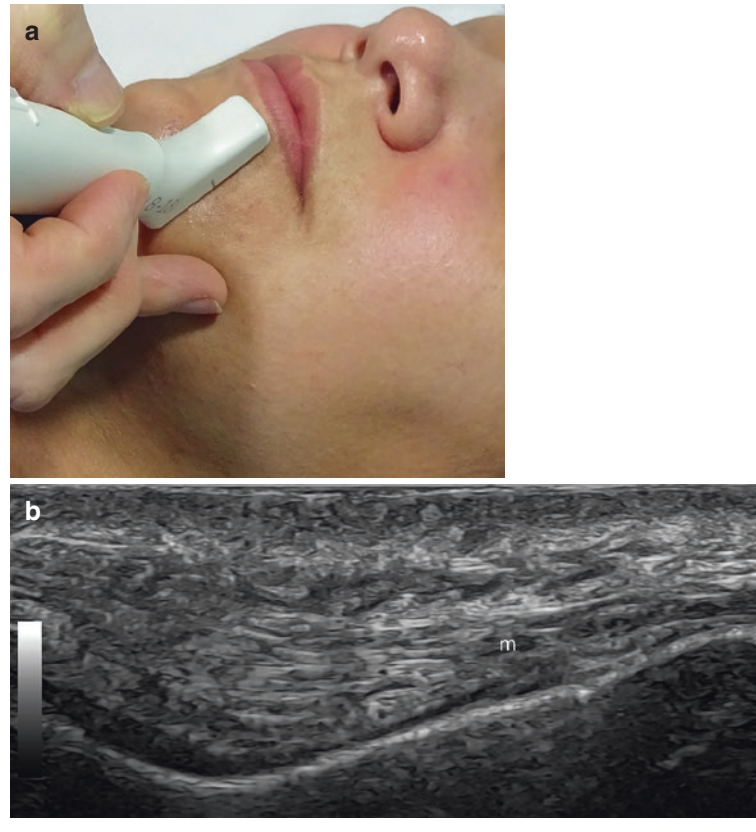

Fig. 6.14 Depressor labii inferioris muscle. (**a**) Clinical image with the probe's position. (**b**) Ultrasound (grayscale; longitudinal view of the muscle) presents the depressor labii inferioris muscle. The depressor anguli oris muscle and the depressor labii inferioris muscle conform a "letter V." The depressor labii inferioris muscle is the medial part of the V

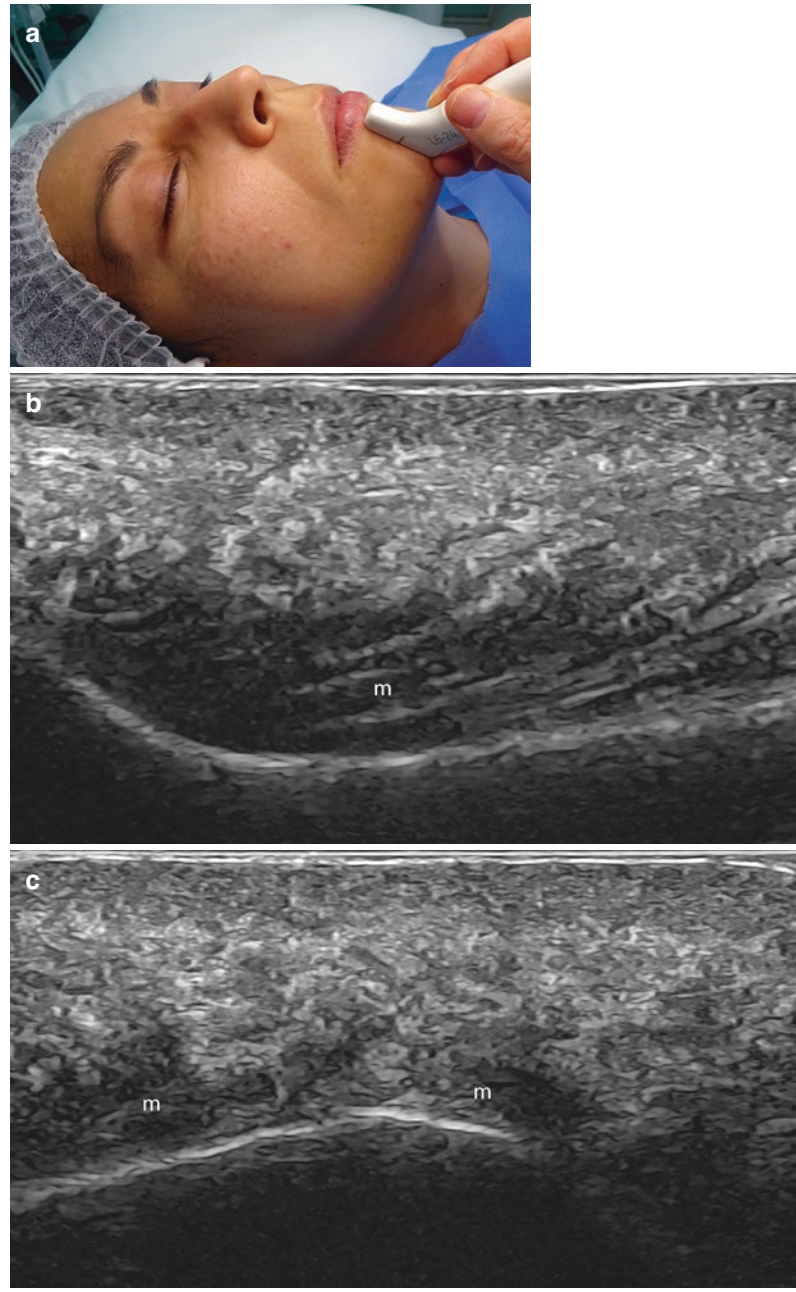

Fig. 6.15 Mentalis muscle. (**a**) Clinical image presents the location of the probe. Ultrasound images (**b**, longitudinal and **c**, transverse views) of the mentalis muscle

Nose

The nose has three areas with different echostructure. All of them present the skin layers as previously described; however, the hypodermis does not present as prominent fatty lobules, and it is more a fibroadipose layer. The dermis is thicker in the tip and slightly more hypoechoic in comparison with the proximal and middle parts.

The proximal part contains the two hypoechoic longitudinal bands given by the procerus muscles. Underneath, in the proximal part, there is a convex hyperechoic layer that is generated by the nasal bones.

In the dorsum, there is a paired muscle called the nasalis muscle, which appears as a very thin, almost perceptible, hypoechoic layer in most patients. This muscle has two parts, one mainly

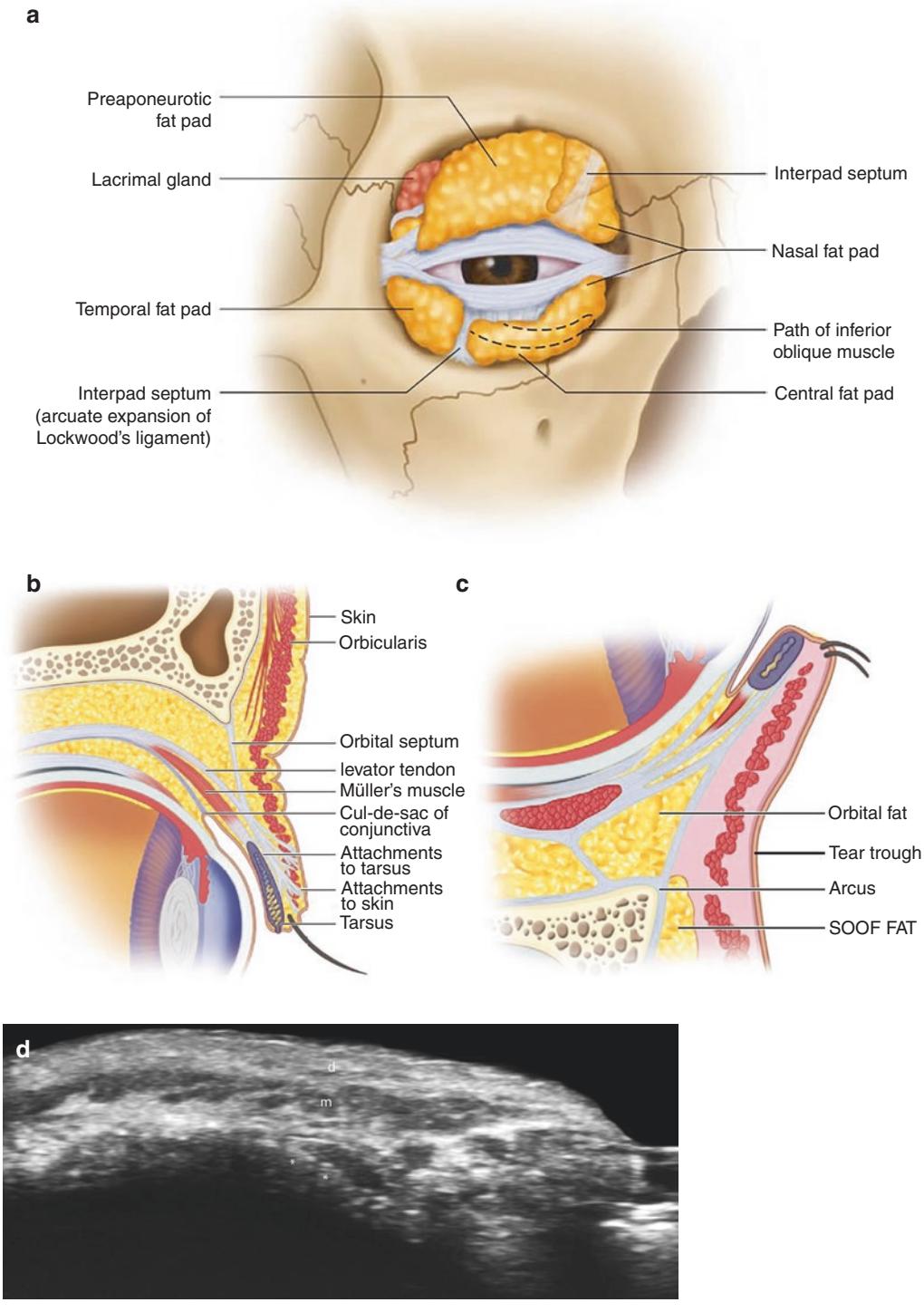

Fig. 6.16 Drawings of the anatomy of the orbital fat pads and the eyelids and ultrasound anatomy of the upper eyelid at 70 MHz. (**a**) Orbital fat pads. (**b**) Upper eyelid structures. (**c**) Lower eyelid structures. (**d**) Upper eyelid at 70 MHz. Grayscale ultrasound (longitudinal view) shows the layers of the eyelid. Abbreviations: *d* dermis, *m* orbicularis oculi muscle, *SOOF* suborbicularis oculi fat; * tarsal plate with Meibomian glands

in the dorsum called the transverse part and one in the alar region called the alar part. The latter part is also called the dilator naris posterior.

Underneath the nasalis muscle, two band-like hypoechoic convex structures correspond to the superior nasal cartilages.

In the distal part of the nose, also called the tip, the alar nasal cartilages appear as two convex hypoechoic band-like structures.

The cartilages usually are avascular by definition, and the vascularization surrounds the cartilages. The lowest part of the nose's tip is called columella and contains the lower parts of the alar cartilages and mostly fibrous tissue (Figs. 6.17, 6.18, 6.19, 6.20, and 6.21).

The vascularity of the external nose is provided by branches of the facial artery, like the angular, alar, and dorsal nasal arteries. A few

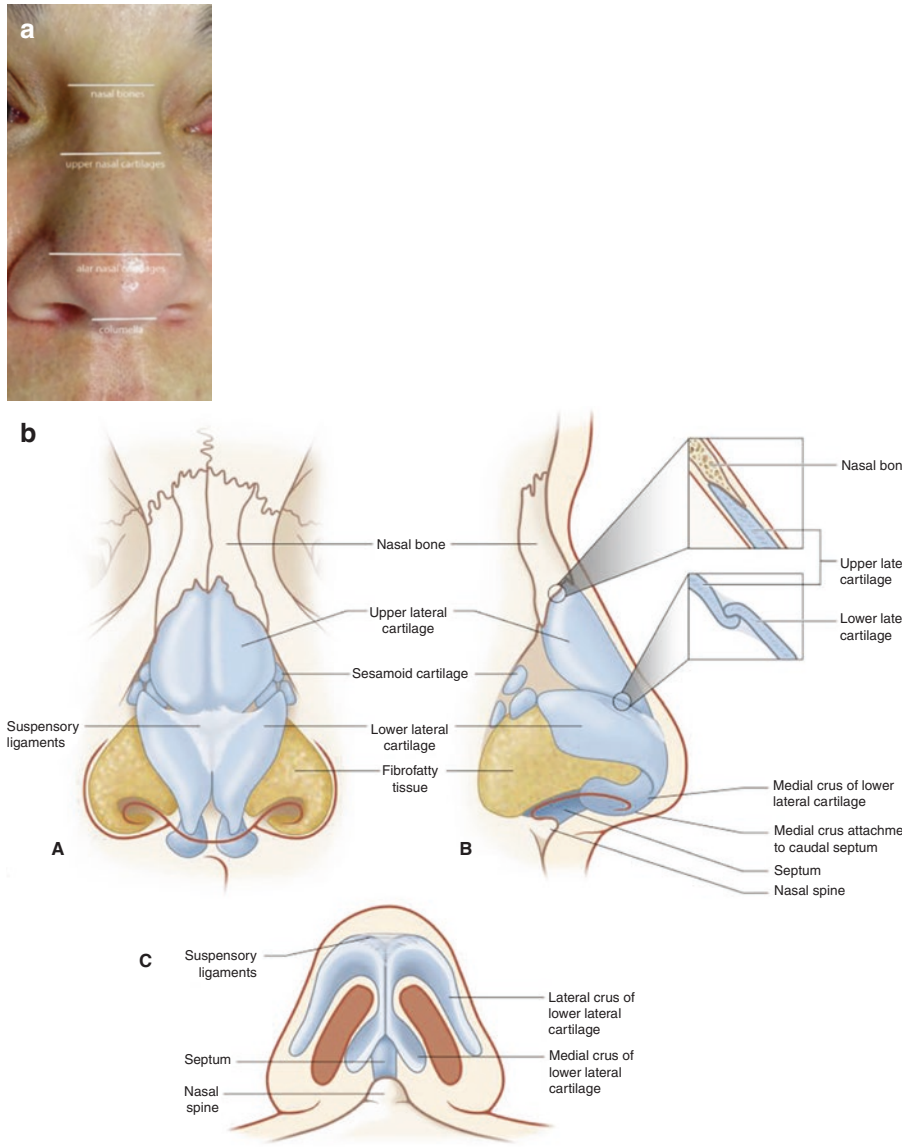

Fig. 6.17 Levels of the nose and drawings of the nasal cartilages. (**a**) Superficial anatomical levels of the nose. (**b**) Drawing of the cartilages of the nose

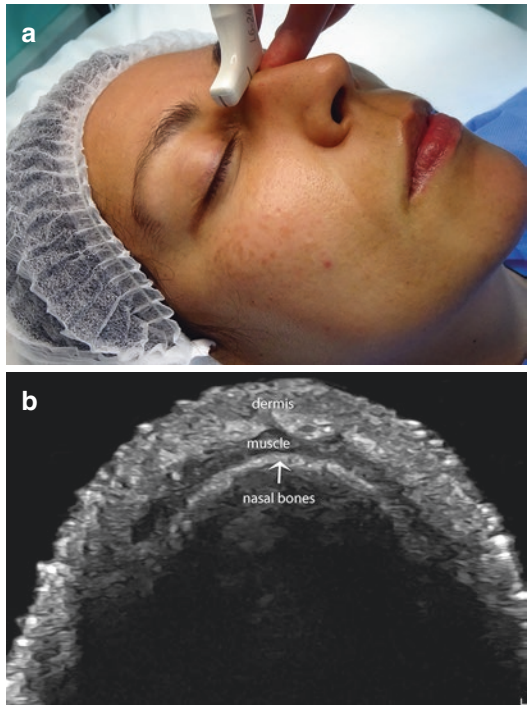

Fig. 6.18 Nasal bones. (**a**) Clinical image presents the probe's location. (**b**) Ultrasound (grayscale, transverse view) demonstrates the nasal bones. On top of the nasal bones are the muscle (procerus muscles) and the dermis

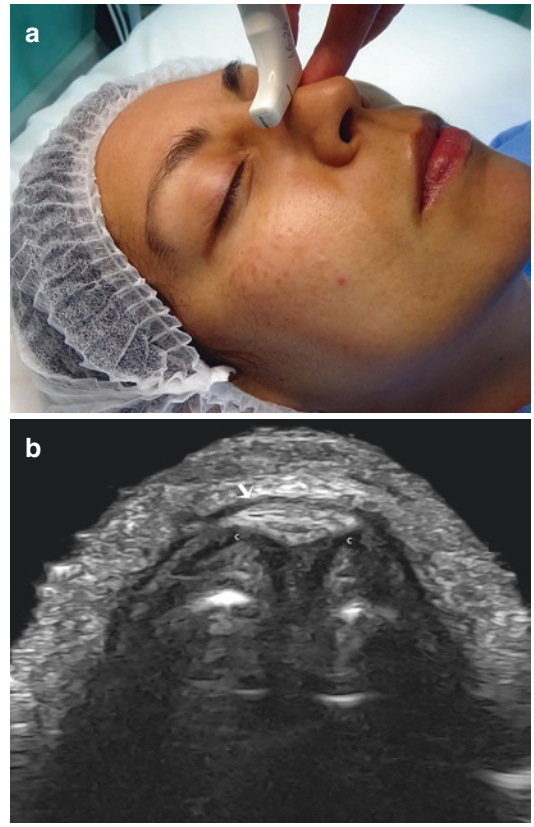

Fig. 6.19 Nasal dorsum. Upper nasal cartilages. (**a**) Clinical photograph shows the probe's position. (**b**) Ultrasound (grayscale, transverse view) presents the upper nasal cartilages (**c**) and the nasalis muscle (arrow)

branches also come from the supraorbital and infraorbital arteries that supply the upper external nose [19–26].

Lips

The upper and lower lips present epidermis and dermis with similar patterns to what has already been described. The orbicularis oris appears as a hypoechoic band located in between the cutaneous and submucosal layers surrounding the mouth's opening.

The vascularity of the lips is provided by the superior and inferior labial arteries that are branches of the facial arteries. These arteries tend to run in the hypodermis of the outer borders and then go deeper to the orbicularis oris muscle [19, 25, 27–30] (Figs. 6.22 and 6.23).

Ear

The ear pinna presents different anatomical layers in the upper two-thirds compared to the lower third, also called the lobule. The main differences are that there is no fatty tissue in the hypodermis in the upper two-thirds, and in the lower third, there is no cartilage.

In the upper two-thirds, the epidermis and dermis show the same echostructure as previously described. The ear cartilage appears as a mixed convex and concave hypoechoic band. The outer prominence of the ear pinna is called the helix and the inner prominence is called the antihelix.

In the lobule, there are epidermis, dermis, and hypodermis that show the well-known features already described. Some hair follicles can also be found in this part, particularly in adults and older persons [19, 26, 29, 31] (Fig. 6.24a–e).

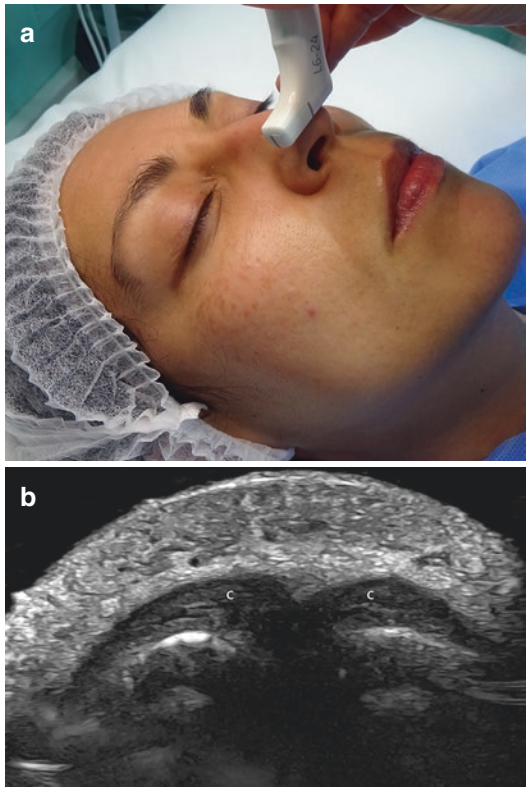

Fig. 6.20 Nasal tip. Alar cartilages. (**a**) Clinical image presents the probe's location. (**b**) Ultrasound image (gray-scale, transverse view) demonstrates the alar cartilages. *c* alar cartilages

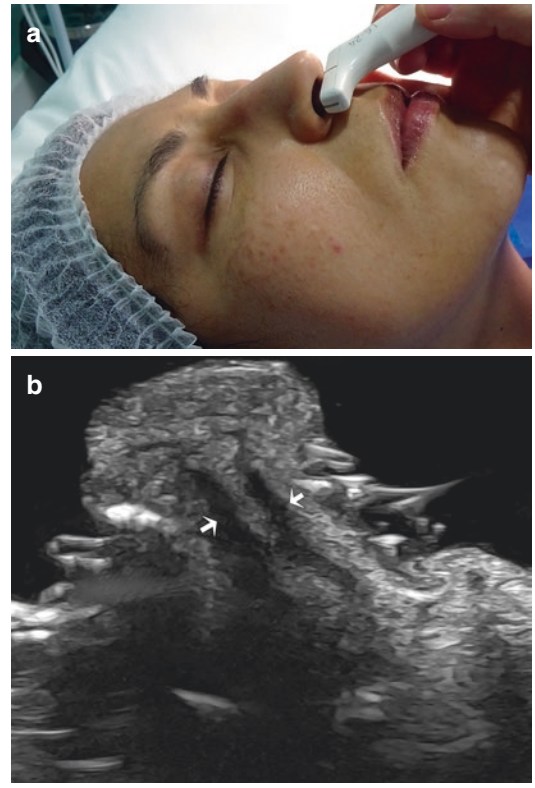

Fig. 6.21 Nasal tip. Columella. (**a**) Clinical image presents the probe's position. (**b**) Ultrasound image (gray-scale, transverse view) demonstrates the inferior part of the alar cartilages (arrows)

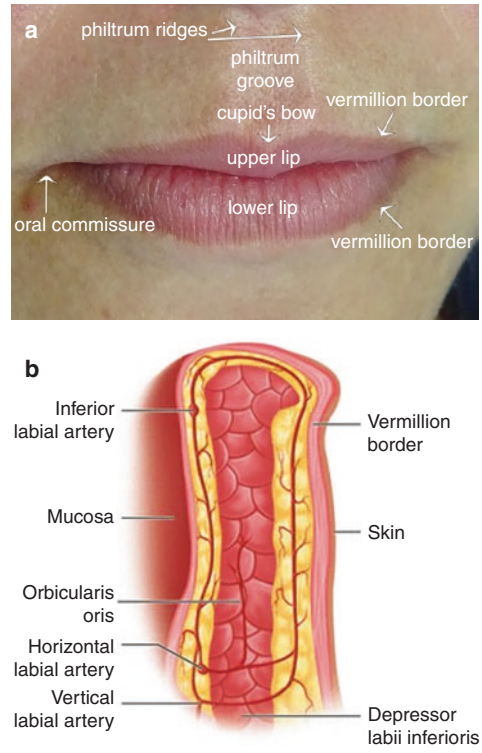

Fig. 6.22 Anatomy of the lips. (**a**) Surface anatomy of the lips. (**b**) Drawing of the anatomy of the lower lip

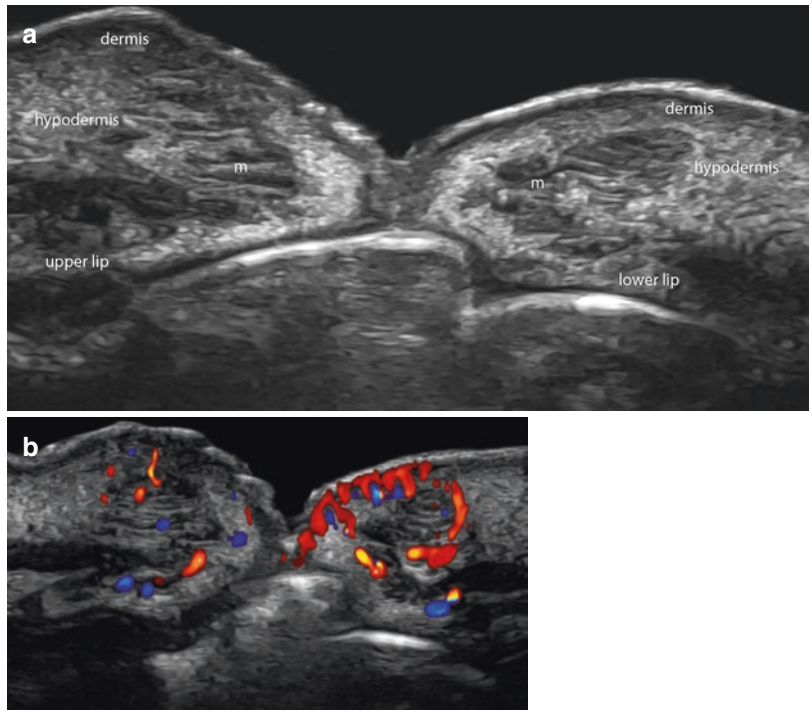

Fig. 6.23 Upper and lower lip ultrasound images (longitudinal views). (**a**) Grayscale and (**b**) color Doppler demonstrate the main layers of the lips and their normal vascularity. Abbreviation: *m* orbicularis oris muscle, * labial arteries

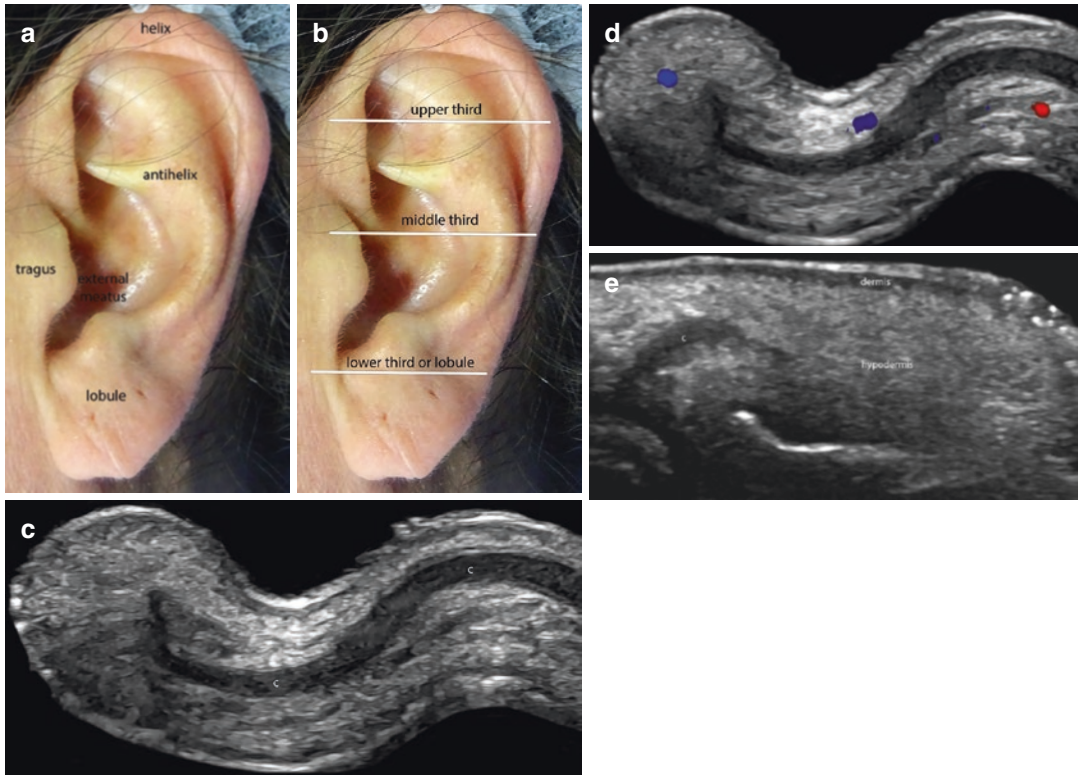

Fig. 6.24 Ear pinna. (**a**) Surface anatomy. (**b**) Levels. (**c**–**e**). Ultrasound images (transverse views). (**c**) upper third, (d) middle third (**c**, grayscale; **d**, color Doppler) and (**e**) lobule (grayscale)

Anatomical Variants

Salivary Glands

Among the most common variants are accessory salivary glands in the cheek, also called accessory parotid glands. These are usually located on top of the upper third of the masseter muscle. Their echogenicity is similar to the parotid gland.

Another variant is the presence of prominent anterior prolongations of the parotid gland that cover the upper third of the masseter muscle.

These glandular variants follow the parotid duct axis and are relevant in aesthetic procedures because these can be injured if the operator does not know their presence [19, 26, 32, 33].

In the oral cavity, several minor salivary glands appear as tiny nodular hypoechoic submucosal structures (Figs. 6.25, 6.26, 6.27, 6.28, and 6.29).

Main Arteries: Facial, Angular, Labial, Alar, Supratrochlear, Supraorbital, Infraorbital

Several arteries present a potential risk for the procedures. Besides, there are multiple variants in the main facial arteries' distribution, presence, and caliber [1, 23, 34–39] (Figs. 6.30, 6.31, 6.32, 6.33, 6.34, 6.35, 6.36, 6.37, 6.38, and 6.39). A tip for finding some of the arteries is to look for the corresponding notch in the bony margin.

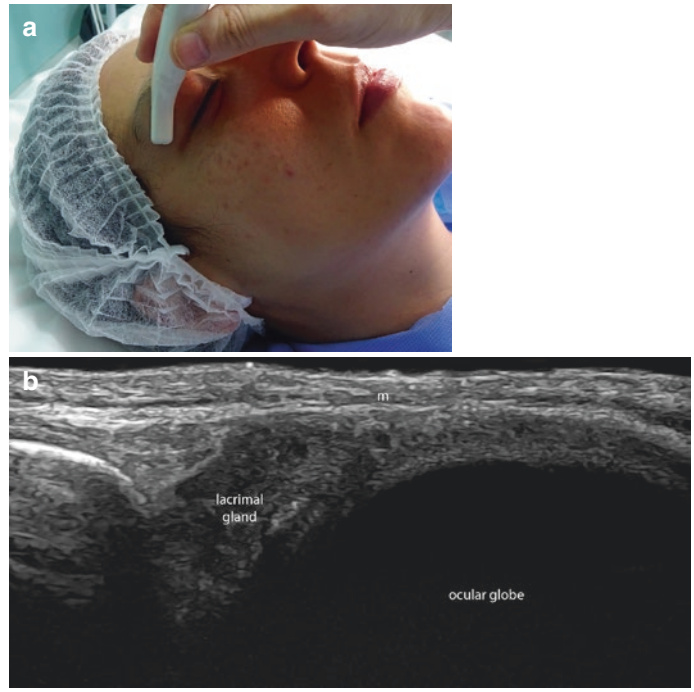

Fig. 6.25 Lacrimal gland. (**a**) Clinical image presents the location of the probe. (**b**) Ultrasound image (grayscale) demonstrates the lacrimal gland. Abbreviation: *m* orbicularis oculi muscle

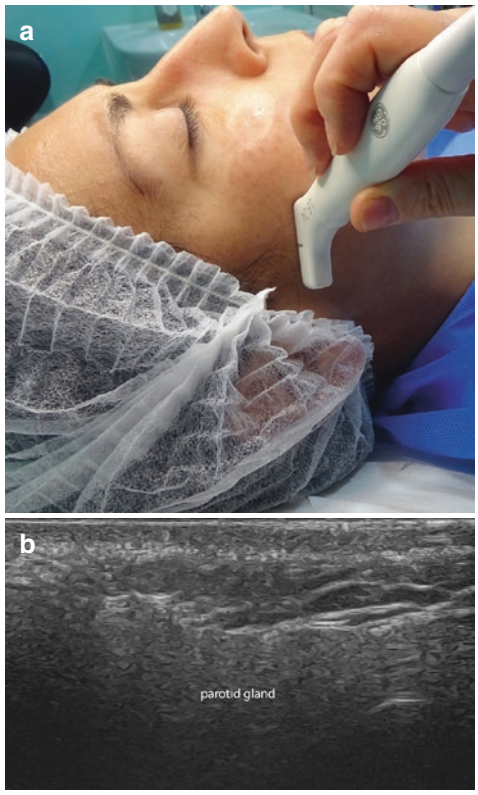

Fig. 6.26 Parotid gland. (**a**) Clinical image demonstrates the position of the probe. (**b**) Ultrasound image (grayscale, transverse view) shows the parotid gland

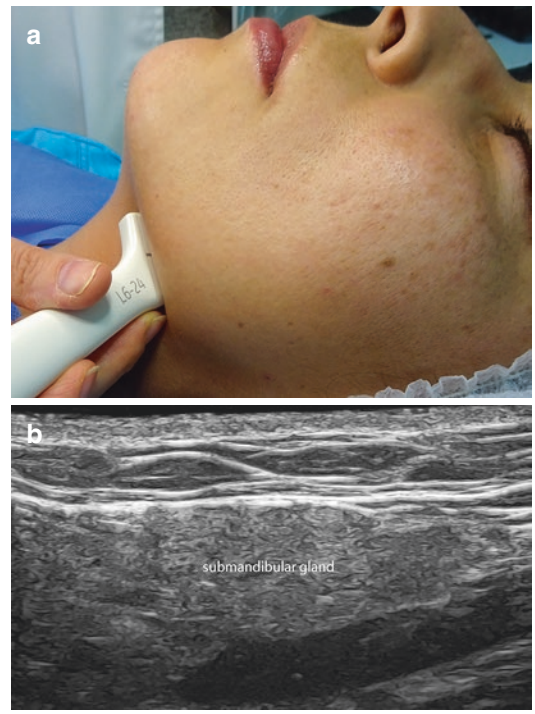

Fig. 6.27 Submandibular gland. (**a**) Clinical photograph presents the probe's location. (**b**) Ultrasound image (grayscale, oblique) demonstrates the submandibular gland

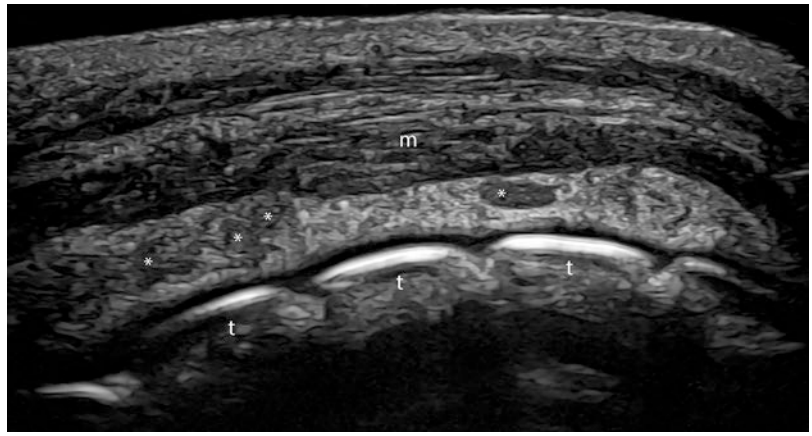

Fig. 6.28 Minor salivary glands. Ultrasound image (grayscale, transverse view, upper lip) shows round and oval-shaped structures (*) that correspond to minor salivary glands located in the submucosal region. Abbreviations: *m* orbicularis oris, *t*, tooth

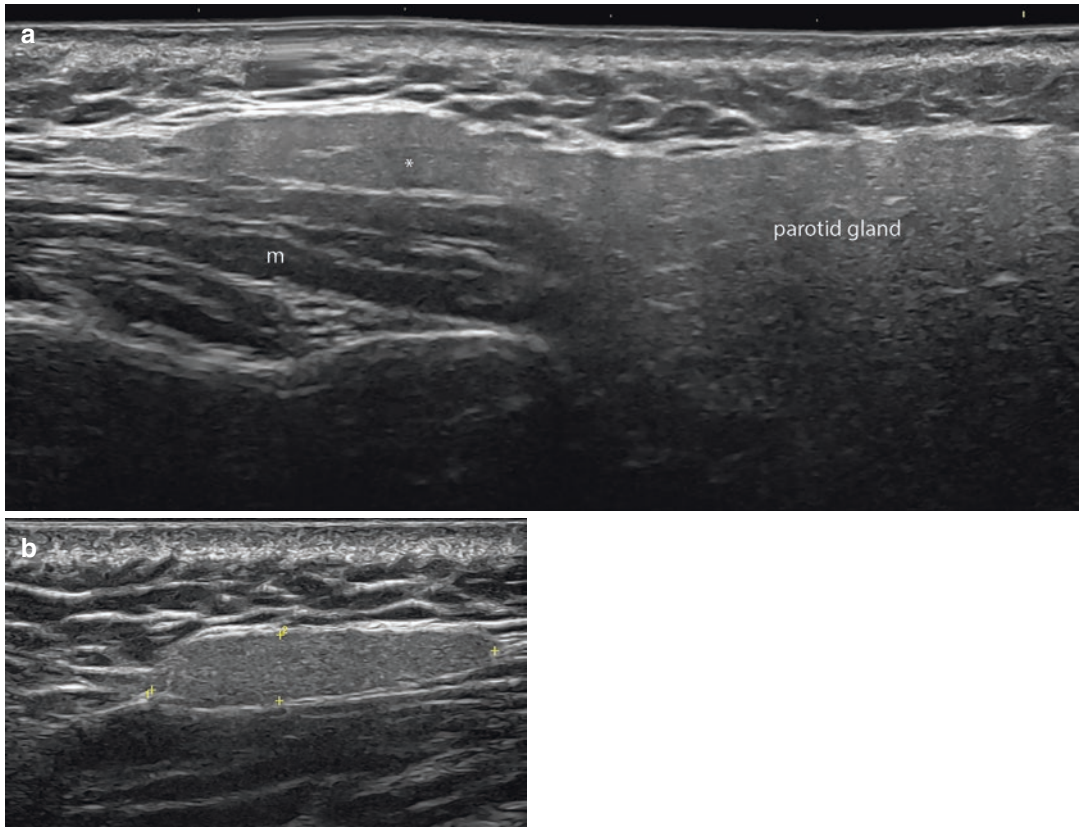

Fig. 6.29 Anatomical variants of the glands (grayscale, transverse views). (**a**) Prominent anterior part (*) of the parotid gland. (**b**) Accessory salivary gland (between markers) located on top of the upper third of the masseter muscle that follows the axis of the parotid duct

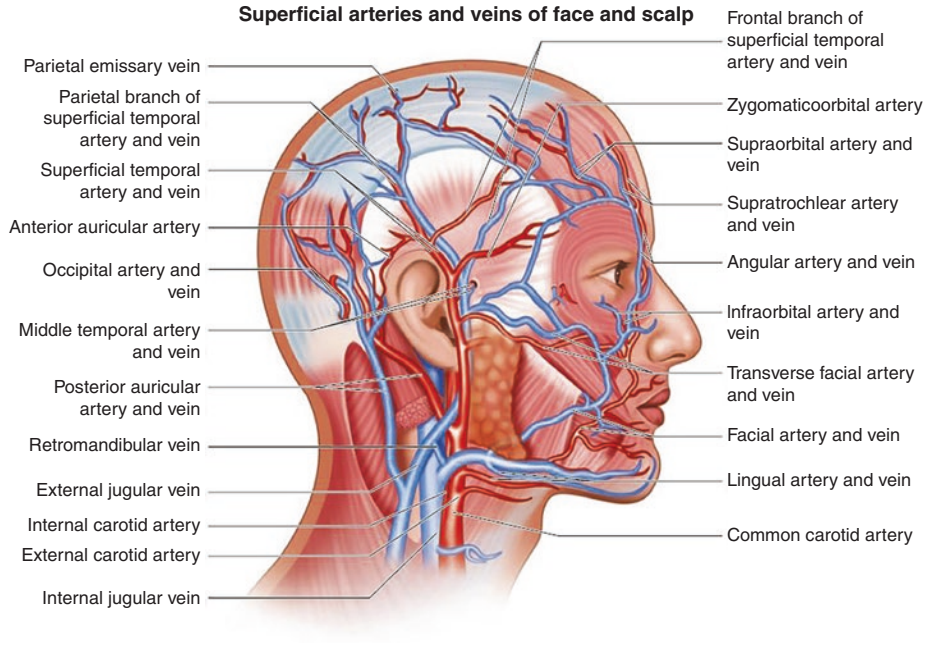

Fig. 6.30 Main vessels of the face and scalp (sagittal view)

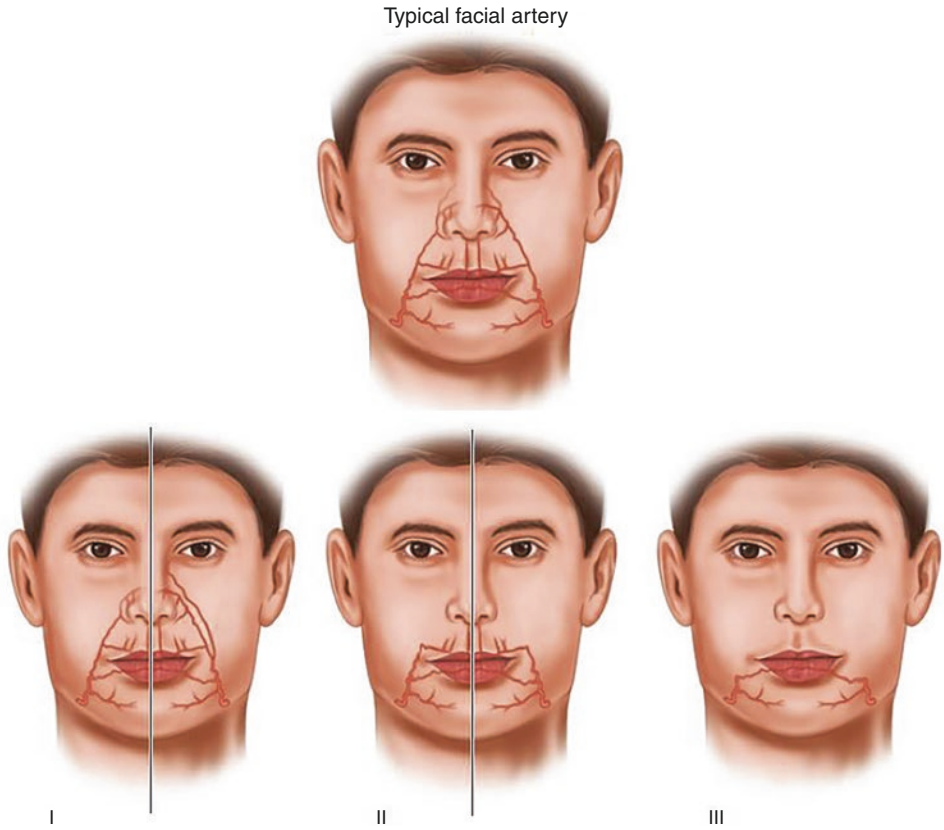

Fig. 6.31 The typical path of the facial and labial arteries and some anatomical variants (I–III)

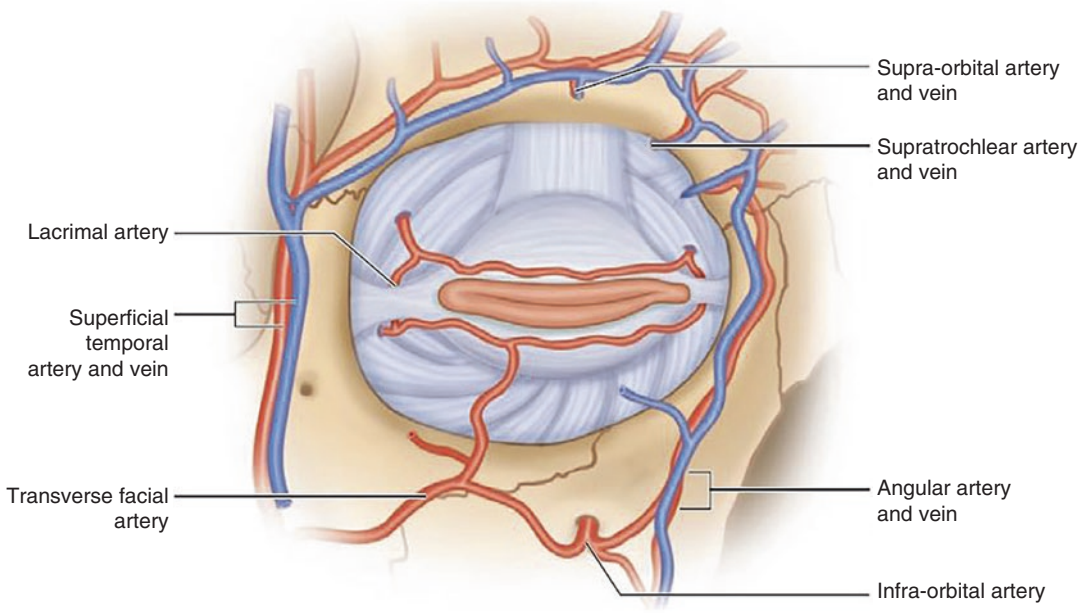

Fig. 6.32 Drawing of the main vessels of the orbit

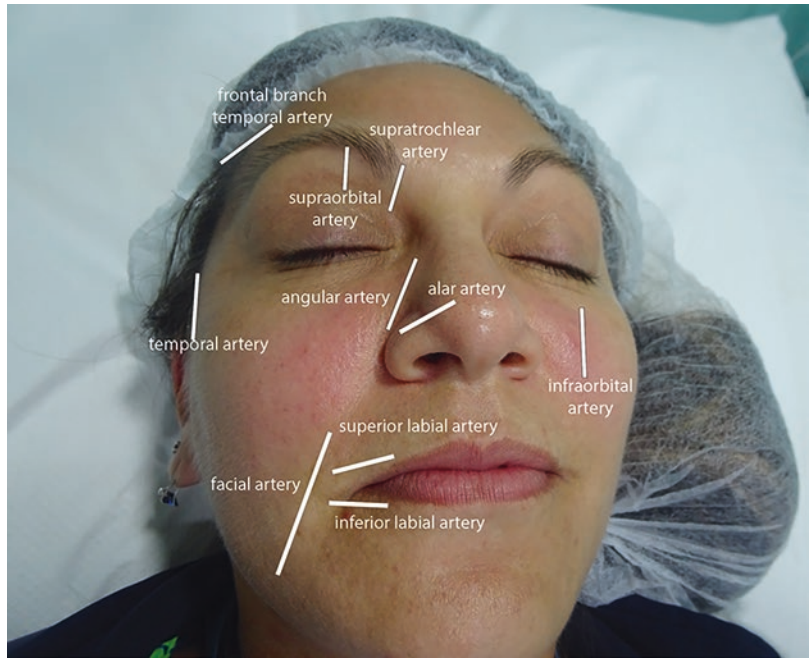

Fig. 6.33 Scheme of the probe positions to scan the main arteries of the face

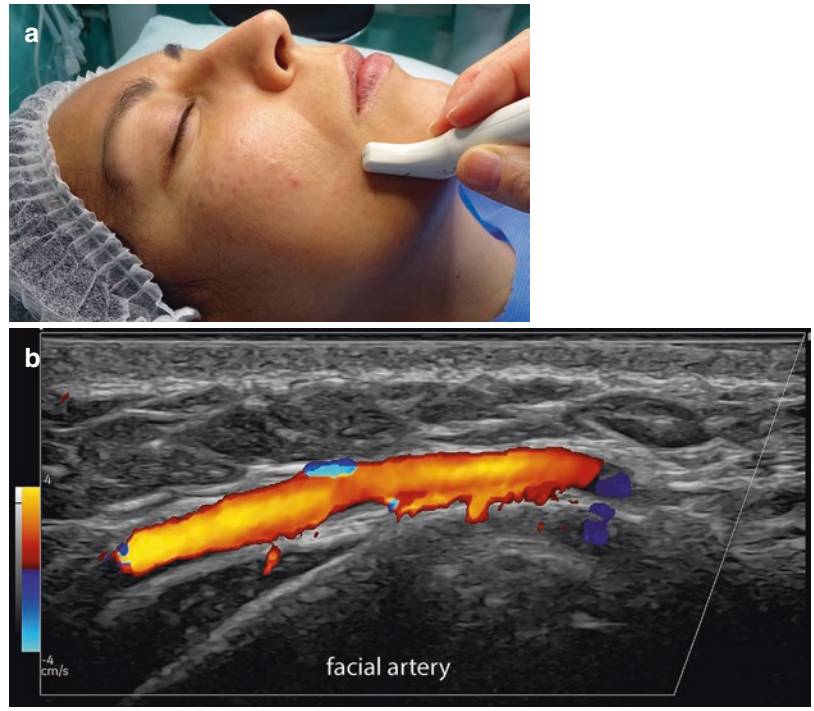

Fig. 6.34 Facial artery. (**a**) Clinical photograph of the probe's position. (**b**) Color Doppler ultrasound image shows the artery in colors

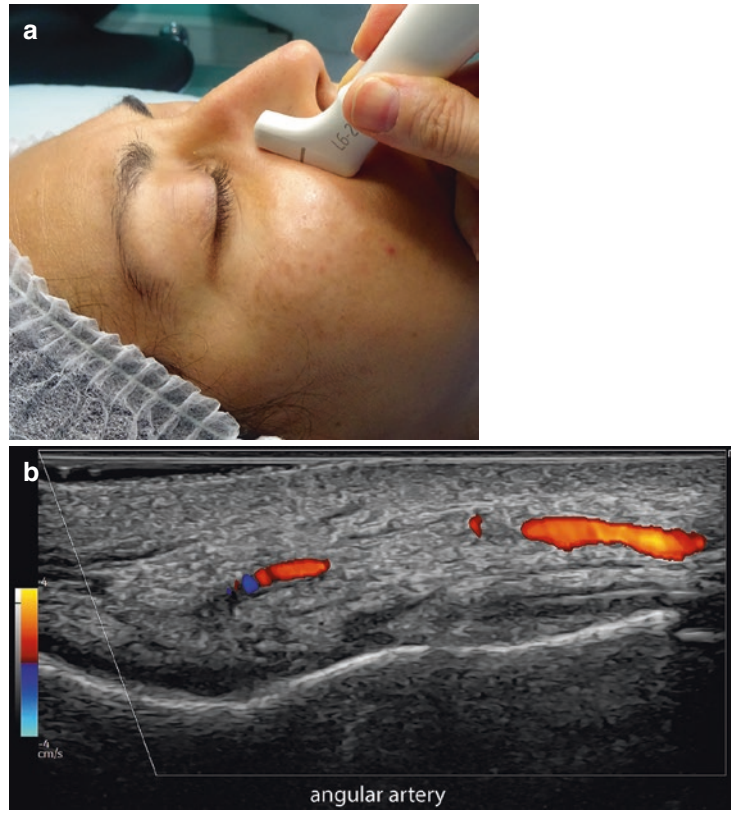

Fig. 6.35 Angular artery. (**a**) Clinical image presents the location of the probe. (**b**) Color Doppler ultrasound image demonstrates the path of the angular artery in colors

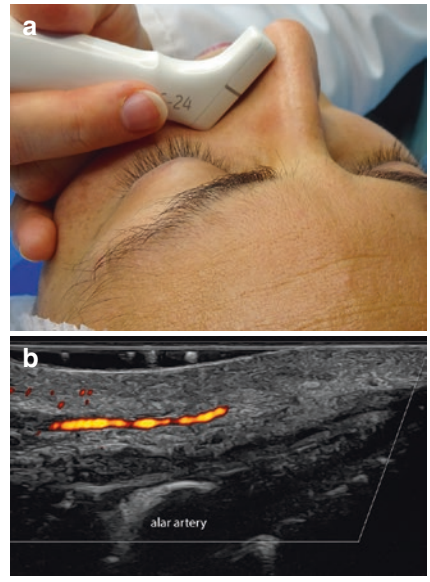

Fig. 6.36 Alar artery. (**a**) Clinical image demonstrates the probe's position. (**b**) Power Doppler ultrasound shows the alar artery (in color)

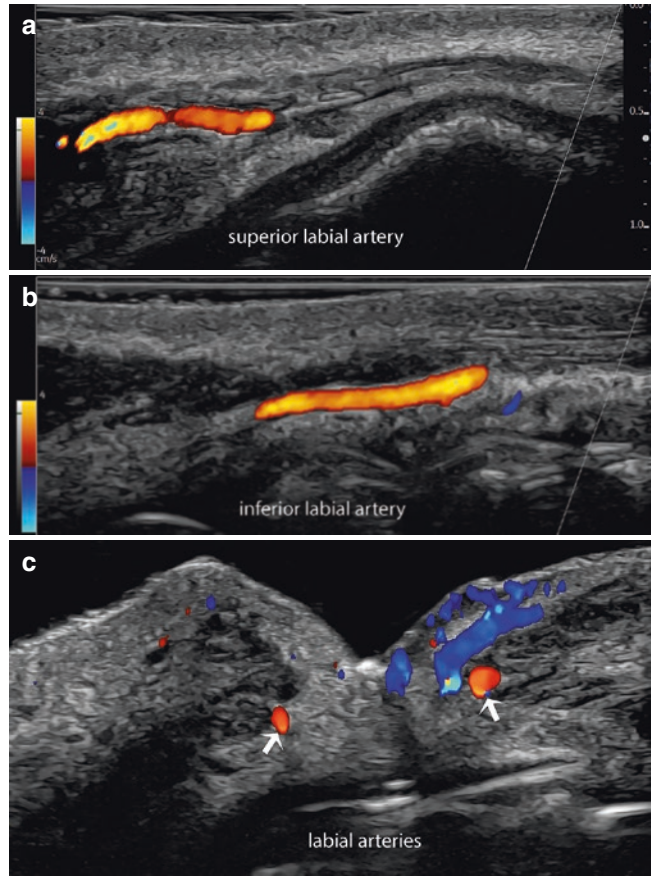

Fig. 6.37 Labial arteries. Color Doppler ultrasound images (**a**, **b**, transverse views, and **c**, longitudinal view) show the superior and inferior labial arteries (arrows in **c**)

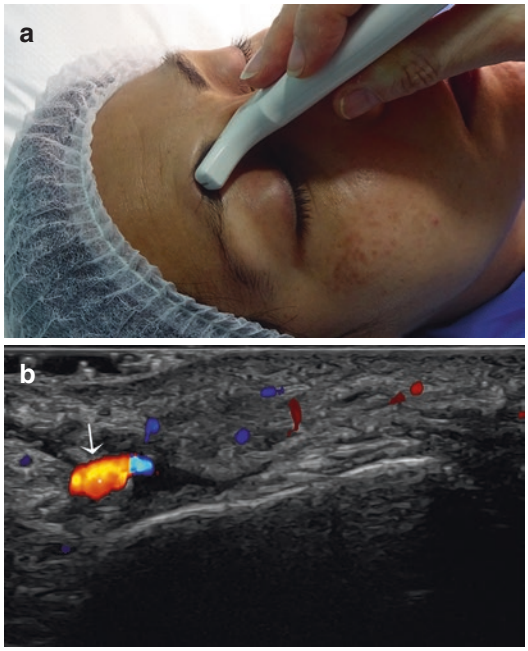

Fig. 6.38 Supratrochlear artery. (**a**) Clinical image presents the probe's location. (**b**) Color Doppler ultrasound image (transverse view) shows the supratrochlear artery (arrow and *)

Fig. 6.39 Supraorbital artery. (**a**) Clinical image presents the probe's position. (**b**) Color Doppler ultrasound image (transverse view) demonstrates the supraorbital artery (arrow and *)

Fig. 6.40 Superficial loop of the facial artery in the peribuccal region. Power Doppler ultrasound (transverse view) demonstrates the loop that brings the artery closer to the dermis

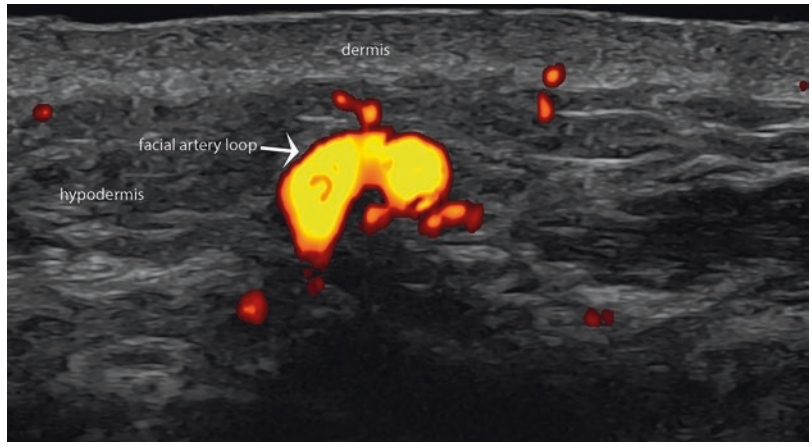

In the peribuccal region, one of the common variants is the superficial loop of the facial artery where this vessel goes towards the skin, usually to the upper hypodermis or to the dermis-hypodermis border (Fig. 6.40).

In the lips, a common variant is the caliber persistent artery, which is a branch that does not taper as the usual arteries when they enter the cutaneous layers [11, 19, 25–27, 37, 40–42] (Fig. 6.41).

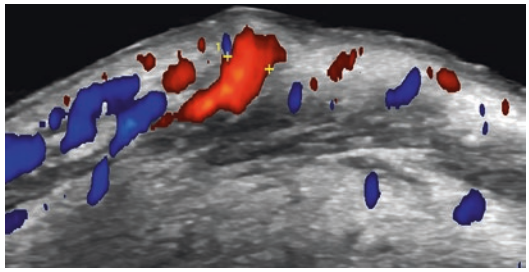

Fig. 6.41 Caliber persistent artery of the lip. Color Doppler ultrasound (transverse view) shows an abnormal thick artery (between markers) in the dermal layer of the lower lip

Relevant Risk Zones of the Head

The head is a complex region, and many anatomical structures could be damaged during procedures. These zones present important vessels or nerves that need to be avoided during cosmetic or surgical procedures [11, 19, 25, 26, 28, 30, 31, 38, 43–45].

Glabellar Region

This region presents the highest rate of major complications, including blindness, because it gathers important and interconnected arteries subject to injury. Among them are the supratrochlear, supraorbital, and dorsal nasal arteries [1, 5, 11, 19, 25, 26, 28, 30, 31, 38, 43–45].

Temple and Lateral Part of the Frontal Region

In this region, the main risk is provided by the injury of the frontal and parietal branches of the temporal artery [1, 5, 11, 19, 25, 26, 28, 31, 38, 43, 45].

Parietotemporal Region

This region shows the parietal branch of the temporal artery that runs in the subaponeurotic layer [1, 5, 11, 19, 24–26, 28, 31, 38, 43, 45].

Preauricular Region

In this region, the main risk is the damage of the temporal vessels, both the artery and the vein. The main facial and trigeminal nerves are difficult to identify on ultrasound [1, 5, 11, 19, 24–26, 28, 31, 38, 43, 45].

Infraorbital Region

This part contains the infraorbital artery that runs close to the bony margin [1, 5, 11, 19, 24–26, 28, 31, 38, 43, 45].

Nasofold Region

In this region, we can identify the angular artery that is a branch of the facial artery. The angular arteries are a continuation of the facial arteries but receive their name after the alar nasal arteries exit. They follow their path through the nasofold lines [1, 5, 11, 19, 24–26, 28, 31, 37, 38, 43, 45].

References

1. Abramo AC, Do Amaral TP, Lessio BP, De Lima GA. Anatomy of forehead, glabellar, nasal and orbital muscles, and their correlation with distinctive patterns of skin lines on the upper third of the face: reviewing concepts. Aesthet Plast Surg. 2016;40(6):962–71.
2. Alfen NV, Gilhuis HJ, Keijzers JP, Pillen S, Van Dijk JP. Quantitative facial muscle ultrasound: feasibility and reproducibility. Muscle Nerve. 2013;48(3):375–80.
3. Bae JH, Choi DY, Lee JG, Seo KK, Tansatit T, Kim HJ. The risorius muscle: anatomic considerations with reference to botulinum neurotoxin injection for masseteric hypertrophy. Dermatol Surg. 2014;40(12):1334–9.
4. Choi YJ, Kim JS, Gil YC, et al. Anatomical considerations regarding the location and boundary of the depressor anguli oris muscle with reference to botulinum toxin injection. Plast Reconstr Surg. 2014;134(5):917–21.
5. Choi YJ, Lee KW, Gil YC, Hu KS, Kim HJ. Ultrasonographic analyses of the forehead region for injectable treatments. Ultrasound Med Biol. 2019;45(10):2641–8.
6. Costin BR, Plesec TP, Sakolsatayadorn N, Rubinstein TJ, McBride JM, Perry JD. Anatomy and histology of

the frontalis muscle. Ophthalmic Plast Reconstr Surg. 2015;31(1):66–72.
7. Hur MS, Hu KS, Park JT, Youn KH, Kim HJ. New anatomical insight of the levator labii superioris alaeque nasi and the transverse part of the nasalis. Surg Radiol Anat. 2010;32(8):753–6.
8. Hur MS, Kim HJ, Choi BY, Hu KS, Kim HJ, Lee KS. Morphology of the mentalis muscle and its relationship with the orbicularis oris and incisivus labii inferioris muscles. J Craniofac Surg. 2013;24(2):602–4.
9. Hwang K, Lee JH, Lim HJ. Anatomy of the corrugator muscle. J Craniofac Surg. 2017;28(2):524–7.
10. Kaya B, Apaydin N, Loukas M, Tubbs RS. The topographic anatomy of the masseteric nerve: a cadaveric study with an emphasis on the effective zone of botulinum toxin a injections in masseter. J Plast Reconstr Aesthet Surg. 2014;67(12):1663–8.
11. Kim H-J, Kim J, Lee H-K, Seo KK. Clinical anatomy of the face for filler and botulinum toxin injection. 1st ed. Singapore: Imprint/Springer Singapore; 2016.
12. Koerte IK, Schroeder AS, Fietzek UM, et al. Muscle atrophy beyond the clinical effect after a single dose of OnabotulinumtoxinA injected in the procerus muscle: a study with magnetic resonance imaging. Dermatol Surg. 2013;39(5):761–5.
13. Olszewski R, Liu Y, Duprez T, Xu TM, Reychler H. Three-dimensional appearance of the lips muscles with three-dimensional isotropic MRI: in vivo study. Int J Comput Assist Radiol Surg. 2009;4(4):349–52.
14. Pessa JE, Zadoo VP, Garza PA, Adrian EK Jr, Dewitt AI, Garza JR. Double or bifid zygomaticus major muscle: anatomy, incidence, and clinical correlation. Clin Anat. 1998;11(5):310–3.
15. Van Holsbeeck M, Introcaso J. Musculoskeletal ultrasound. 3rd ed. New Delhi: Jaypee Brothers Medical; 2016.
16. Volk GF, Pohlmann M, Finkensieper M, Chalmers HJ, Guntinas-Lichius O. 3D-ultrasonography for evaluation of facial muscles in patients with chronic facial palsy or defective healing: a pilot study. BMC Ear Nose Throat Disord. 2014;14:4.
17. Volk GF, Pohlmann M, Sauer M, Finkensieper M, Guntinas-Lichius O. Quantitative ultrasonography of facial muscles in patients with chronic facial palsy. Muscle Nerve. 2014;50(3):358–65.
18. Volk GF, Wystub N, Pohlmann M, Finkensieper M, Chalmers HJ, Guntinas-Lichius O. Quantitative ultrasonography of facial muscles. Muscle Nerve. 2013;47(6):878–83.
19. Wortsman X. Atlas of dermatologic ultrasound. 1st ed. New York, NY: Springer International Publishing; 2018.
20. Mostafa BE, Elsamny TA, Youssef TA, Elserwi AB, Teaima AA. Arterial blood supply of the nose: an angiographic study. ORL J Otorhinolaryngol Relat Spec. 2018;80(5–6):238–47.
21. Pilsl U, Anderhuber F. The external nose: the nasal arteries and their course in relation to the nasolabial fold and groove. Plast Reconstr Surg. 2016;138(5):830e–5e.
22. Saban Y. Rhinoplasty: lessons from "errors": from anatomy and experience to the concept of sequential primary rhinoplasty. HNO. 2018;66(1):15–25.
23. Toriumi DM, Mueller RA, Grosch T, Bhattacharyya TK, Larrabee WF Jr. Vascular anatomy of the nose and the external rhinoplasty approach. Arch Otolaryngol Head Neck Surg. 1996;122(1):24–34.
24. Tucunduva MJ, Tucunduva-Neto R, Saieg M, Costa AL, de Freitas C. Vascular mapping of the face: B-mode and doppler ultrasonography study. Med Oral Patol Oral Cir Bucal. 2016;21(2):e135–41.
25. von Arx T, Tamura K, Yukiya O, Lozanoff S. The face – a vascular perspective. A literature review. Swiss Dent J. 2018;128(5):382–92.
26. Wortsman X, Jemec GBE. Dermatologic ultrasound with clinical and histologic correlations. 1st ed. New York, NY: Springer-Verlag; 2013.
27. Cotofana S, Pretterklieber B, Lucius R, et al. Distribution pattern of the superior and inferior labial arteries: impact for safe upper and lower lip augmentation procedures. Plast Reconstr Surg. 2017;139(5):1075–82.
28. Duisit J, Maistriaux L, Gerdom A, et al. Nose and lip graft variants: a subunit anatomical study. Plast Reconstr Surg. 2018;141(3):751–61.
29. Wortsman X, Jemec GB. Sonography of the ear pinna. J Ultrasound Med. 2008;27(5):761–70.
30. Wu SQ, Pan BL, An Y, An JX, Chen LJ, Li D. Lip morphology and aesthetics: study review and prospects in plastic surgery. Aesthet Plast Surg. 2019;43(3):637–43.
31. Szymanski A, Geiger Z. Anatomy, head and neck, ear. Treasure Island (FL): StatPearls. StatPearls Publishing Copyright © 2021, StatPearls Publishing LLC; 2021.
32. Quezada-Gaon N, Wortsman X, Peñaloza O, Carrasco JE. Comparison of clinical marking and ultrasound-guided injection of botulinum type a toxin into the masseter muscles for treating bruxism and its cosmetic effects. J Cosmet Dermatol. 2016;15(3):238–44.
33. Wortsman X, Wortsman J. Sonographic outcomes of cosmetic procedures. AJR Am J Roentgenol. 2011;197(5):W910–8.
34. Koziej M, Polak J, Hołda J, et al. The arteries of the central forehead: implications for facial plastic surgery. Aesthet Surg J. 2020;40(10):1043–50.
35. Koziej M, Trybus M, Hołda M, et al. Anatomical map of the facial artery for facial reconstruction and aesthetic procedures. Aesthet Surg J. 2019;39(11):1151–62.
36. Koziej M, Trybus M, Hołda M, et al. The superficial temporal artery: anatomical map for facial reconstruction and aesthetic procedures. Aesthet Surg J. 2019;39(8):815–23.
37. Lasjaunias P, Berenstein A, Doyon D. Normal functional anatomy of the facial artery. Radiology. 1979;133(3 Pt 1):631–8.
38. Scheuer JF 3rd, Sieber DA, Pezeshk RA, Gassman AA, Campbell CF, Rohrich RJ. Facial danger zones:

techniques to maximize safety during soft-tissue filler injections. Plast Reconstr Surg. 2017;139(5):1103–8.
39. Tucker SM, Linberg JV. Vascular anatomy of the eyelids. Ophthalmology. 1994;101(6):1118–21.
40. Arellano J, Antoniazzi C, Wortsman X. Early diagnosis of a calibre persistent labial artery in a child: usefulness of ultrasonography. Australas J Dermatol. 2012;53(2):e18–9.
41. Lohn JW, Penn JW, Norton J, Butler PE. The course and variation of the facial artery and vein: implications for facial transplantation and facial surgery. Ann Plast Surg. 2011;67(2):184–8.
42. Wortsman X, Calderón P, Arellano J, Orellana Y. High-resolution color Doppler ultrasound of a caliber-persistent artery of the lip, a simulator variant of dermatologic disease: case report and sonographic findings. Int J Dermatol. 2009;48(8):830–3.
43. Ferneini EM, Hapelas S, Watras J, Ferneini AM, Weyman D, Fewins J. Surgeon's guide to facial soft tissue filler injections: relevant anatomy and safety considerations. J Oral Maxillofac Surg. 2017;75(12):2667.e2661–5.
44. Tansatit T, Apinuntrum P, Phetudom T. Cadaveric assessment of lip injections: locating the serious threats. Aesthet Plast Surg. 2017;41(2):430–40.
45. Wollina U, Goldman A. Facial vascular danger zones for filler injections. Dermatol Ther. 2020;33(6):e14285.